

Mapping Inter-City Trade Networks to Maximum Entropy Models using Electronic Invoice Data

Cesar I. N. Sampaio Filho,^{1,2} Rilder S. Pires,^{3,2}

Humberto A. Carmona,^{1,2} and José S. Andrade Jr.^{1,2,*}

¹*Departamento de Física, Universidade Federal do Ceará,
60451-970 Fortaleza, Ceará, Brazil*

²*Centro de Análise de Dados e Avaliação de Políticas Públicas,
Instituto de Pesquisa e Estratégia Econômica do Ceará,
60822-325, Fortaleza, Ceará, Brazil*

³*Laboratório de Ciência de Dados e Inteligência Artificial,
Universidade de Fortaleza, 60811-905 Fortaleza, Ceará, Brazil*

(Dated: July 19, 2024)

Abstract

We analyze the network of transactions among cities based on the electronic invoice database for the municipalities in the Ceará state, Brazil. This database consists of approximately 3.7 billion records, each containing 43 fields of information, registered during the period between the years 2016 to 2019. All the transactions are grouped in a unique dataset and represented as an asymmetrical adjacency matrix corresponding to a directed graph with connections weighted by the number of transactions among cities. Due to the large size of Ceará state, $148,894.442 \text{ km}^2$ [1], its unequal distribution of wealth, and spatially heterogeneous population density, we initially determine communities of cities based on their mutual intensity of trades and then verify to which extent their economic interests somehow reflect what we define as a “community cohesiveness”. For the first task, we use the Infomap algorithm to detect the partition which provides the shortest description length and captures the optimal community structure of the network in terms of its associated flow dynamics. Surprisingly, the partition identified has five modules, whose two-dimensional geographical projections are all simply-connected domains, *i.e.*, consisting of single pieces without holes. Having described the topological properties of the transaction network, we proceed with the analysis of our database from the perspective of traded products by building bipartite structures represented in terms of adjacency matrices between municipalities and products, considering both the contexts of selling and buying. We then make use of the revealed comparative advantage (RCA) concept, widely used in foreign trade analyses, to define a non-monetary and binary activity index that is capable to distinguish the relative advantage of a city in a class of goods or services as evidenced by trade flows. Finally, through the pairwise Maximum Entropy Model, we can associate to the largest communities previously characterized, their corresponding binary Ising-like Hamiltonian models. The local fields and couplings computed for a given community are those that best reproduce the average product activities of its cities as well as the statistical correlations between the product activities of all pairs of its cities. In an analogy with critical phenomena, our results reveal that each community operates at a “temperature” that is close to the corresponding “critical point”, suggesting a high degree of “economic cohesiveness” in its trade network of cities.

* soares@fisica.ufc.br

I. INTRODUCTION

Economic geography investigates the way different regions and countries are interconnected through trade and investment, as well as how these relationships affect growth, development and inequality. Understanding the complex relationships between the enormous number of economic activities, people, firms and places requires the definition of metrics necessarily involving dimensionality reduction techniques that together are referred to as Economic Complexity (EC). The Economic Complexity Index (ECI) [2, 3] and the Economic Fitness Index (EFI) [4, 5] are two examples of these metrics. Both of them are based on the examination of the intrinsic interdependencies between countries and regions by exploring international trade data. In this way, researchers have gained insight, for example, into which countries are important hubs in global trade network, how products can be compared in terms of their relative complexity and distinctiveness. Through the concept of *proximity* between products, Hidalgo and Hausmann [6] proposed that the export basket of developing countries should expand more efficiently, from an economical point of view, to new products that are “close” to the ones already being exported.

One key concept present in all these approaches is that the rarity of the products a country exports, their technological complexity and diversity should be closely related to the country’s installed infrastructure, such as transportation network, energy systems and intellectual capital [2, 4]. Using the index Revealed Comparative Advantage (RCA) [7] to construct a bipartite network of countries and products, it is possible to quantify the complexity and diversity of products, so that countries exports baskets and their Gross Domestic Product (GDP) per capita can be empirically related, aiming to forecast countries growth [2, 4, 5]. However, it is important to note that there are many other factors influencing a country’s GDP per capita, including, for example, its natural resources, political stability, extreme events and more. In this way, while the export basket indeed represents a crucial factor impacting economic growth, it is certainly not the only one.

In Ref. [8] the authors review how machine learning techniques apply to economics with the goal of understanding the systemic interactions that influence various socioeconomic outcomes, and discuss how big data and machine learning are instrumental in this emerging field of economic complexity. Brummitt et al. [9] introduced a machine learning technique, which they named Principal Smooth-Dynamics Analysis (PriSDA), to explore the dynamics

of economic growth. Their findings emphasized that product diversity, particularly in more sophisticated products, serves as a significant driver of income growth. In a parallel vein, Alhora et al. [10] employed supervised learning techniques on the UN-COMTRADE database, using the Harmonized System 1992 classification (HS) [11, 12]. Their research highlights that the ability to forecast the introduction of new products is essential for effective economic planning. In Ref. [13], the authors introduce a novel approach by applying convolutional neural networks to high-resolution satellite imagery. This method is used to estimate economic livelihood indicators, such as consumption expenditure and asset wealth, in five developing African countries: Nigeria, Tanzania, Uganda, Malawi, and Rwanda.

Although EC metrics were initially proposed based on international trade data, they were further developed and applied to non-export data sets and subnational entities. Operti et al. [14] introduced a novel algorithm they termed Exogenous Fitness, as an evolved form of the previously established Fitness metric [15]. Focused on Brazilian states, they assessed regional competitiveness through the export basket. By combining Exogenous Fitness scores with GDP per capita, the authors distinguish between two economic regimes among these states: one with high predictability and another with low predictability. The study also compares Exogenous Fitness rankings to those from Endogenous Fitness and the Economic Complexity Index, offering a comprehensive view of regional economic dynamics.

In this work we apply concepts of EC in the scale of municipalities using electronic invoice trade data. To make an analogy with international trade, we treat sales from one municipality to others as exports. One relevant consideration that naturally arises is that, at this scale, it is not guaranteed that the traded products are in fact produced locally. As a consequence, the spatial correlations at the state level between exports and installed capabilities is expectedly weaker, which led us to approach the trade network from a partitioned point of view, *i.e.*, by considering the potential formation of communities. Community structure plays a pivotal role in understanding the intricate dynamics of complex networks, encompassing diverse domains such as social and biological networks. Its significance lies in the substantial implications it holds for the propagation of information, distribution of resources, and spreading of influence within the network [16–18]. In this study, we initially investigate the phenomenon of community formation induced by the exchange of products between municipalities in the trade network. By examining this interplay, we aim to shed light on the underlying mechanisms by which the “flow” of products induces the formation of communities.

Further, in order to understand the economic patterns commercial activities at the scale of cities, we infer “pairwise interactions” between pair of cities through the products they trade. Particularly, using the binary municipality-product matrices of the communities detected from the network of transactions, we find that often the product baskets of different cities are strongly correlated, both for sales and purchases. We therefore exploit these statistical correlations and the average activities of the cities using the Maximum Entropy Model (MEM) developed in information theory. This method provides a conceptual framework based on statistical physics models for representing a given natural process in terms of “interactions” between its elementary units using experimental data [19]. More precisely, the principle of maximum entropy encapsulates the core concept behind the Inverse Ising Problem solution, or the so-called Boltzmann machine, wherein an underlying “Hamiltonian” associated with a given complex system can be inferred from the observed statistical correlations among its constituent parts. In this way, MEM has been applied to systems that can be mapped to Ising-like models, that is, models in which the interacting elements are in an active or inactive state, *i.e.*, a network of moments of dipole with states of spins that are up or down under the action of an external field and their mutual interactions. In a neuronal network, for example, interactions between pairs of neurons that react to some stimuli are deduced from their firing patterns [20–26]. MEM have also been successful in the characterization of protein-protein interactions [27, 28] and genetic interaction networks from gene expression patterns [29–31]. Other complex systems have been analyzed in terms of the Boltzmann machine, for example the collective responses exhibited by flocks of birds [32, 33] and, more recently, the emergence of collective behavior from the eye movement patterns of a group of people while watching commercial videos [34] or reading texts [35].

In Ref. [36], Bury conducts an analysis of stock market data utilizing a maximum entropy model. Within this framework, market indices are conceptualized as time-dependent binary spin states, each characterized by either bullish or bearish behavior. The author focuses on two distinct financial systems: one that encompasses eight European indices, and another that consists of a selection of stocks from the Dow Jones index. Employing criteria outlined in Ref. [37], the presence of criticality in these finite systems is investigated. Specifically, a system is deemed to be approaching a critical state if a peak is observed in the temperature-dependent variance of the likelihood, also known as the heat capacity, near its operational point. The study concludes that neither system functions in a strictly critical state. The

European indices generally operate in proximity criticality, except during market downturns. In contrast, the Dow Jones system is found to function significantly far from criticality.

This paper is organized as follows. In Section II, we present the network of transactions between municipalities in the Ceará state, in the Northeast of Brazil. In Section III, we employ a community detection scheme based on the flow dynamics in the network of transactions to identify regions in the state that are organized by the strength of the local trade quantified by the number of commercial transactions between different municipalities. In Section IV, we apply the MEM to investigate the internal “cohesiveness” of the largest communities focusing on the Ising-like models deduced from the product baskets for sales and purchases of their corresponding cities. Finally, in Section V we present the general conclusions of the work.

II. NETWORKS OF TRANSACTIONS

The Ceará state, in northeaster Brazil, has 184 municipalities, with an estimated population of 9,240,580 people. The network of transactions between pair of cities in Ceará is built from a database of all electronic invoices [38] registered in the state between the years 2016 to 2019, which contains approximately 3.7 billion records, each one corresponding to a traded product, with 43 fields of information. Precisely, we consider all the transactions of products that the cities in Ceará carried out among themselves and with the other cities of Brazil, thus disregarding all transactions circumscribed to a given city. We then applied a thorough process of standardizing and sanitizing the data and deflated all monetary values starting from January 2016, corresponding to our database’s first month. Furthermore, we only considered transactions with values larger than 2000 USD. Once these preprocessing steps are completed, we group all the transactions in a unique dataset and build an asymmetrical adjacency matrix corresponding to a directed graph with connections weighted by the number of transactions between pair of cities.

At this point, with the purpose of characterizing the economic dynamics of the Ceará state in the time window from 2016 to 2019, we proceed with the definition of a complex network based on the data of only internal sales and purchase operations among cities. The network corresponds to a unique, densely connected component with $C = 185$ nodes representing the municipalities, and 14479 directed-weighted edges. The direction of the edge is from

the city that sells to the city that buys one or more given products. To each directed edge between a pair of cities i and j , a weight is associated which corresponds to the total number of sells (buys), n_{ij} , or buys (sells), n_{ji} , operations from i (j) to j (i) performed during the time window. From this network, we can then compute the numbers of internal selling and internal buying connections of each city i , k_i^S and k_i^B , respectively, as well as the sum of their corresponding weights, $W_i^S = \sum_{j=1}^{k_i^S} n_{ij}$ and $W_i^B = \sum_{j=1}^{k_i^B} n_{ji}$.

Figures 1b and 1c show the dependence of the weights of the nodes on their degrees in a double logarithmic plot. As depicted, the relationship between these two variables seems to be well described in terms of a power-law model for both the selling and the buying data sets. In order to attenuate the effect of dispersion of the data points on the parameter estimation, we utilized the RANSAC algorithm [39, 40], which statistically identifies the outliers and fits the model considering only the inlier points. Therefore, among the data points obtained for all cities relating the total number of their internal sales transactions (out-transactions), W^S , with the total number of their internal sales connections (out-degree), k^S , we select only the inliers (green circles) to perform a least-squares fit to the power law, $W^S \simeq (k^S)^\beta$, and find the exponent $\beta = 1.87 \pm 0.03$. Following the same procedure for the inliers in the plot of the in-transactions, W^B , against the in-degree, k^B , the least-squares fit to the power-law, $W^B \simeq (k^B)^\beta$, gives the exponent $\beta = 2.19 \pm 0.01$. The values of these exponents imply that the weights of the cities' connections grow disproportionately faster than their corresponding degrees. Such a superlinear scaling behavior contrasts with the linear one, $W(k) \sim k$, expected for the case in which the weights of the edges n are statistically uncorrelated with the degree of the nodes from where they depart (selling) or to where they arrive (buying) [41–44]. In order to illustrate this condition, we performed additional calculations preserving the degrees of each node i , k_i^S and k_i^B , but shuffling the values of the weights n_{ij} between randomly chosen pairs of edges in the network. In this way, strong correlations, if present in the original network, should disappear. Indeed, the results shown in Fig. ?? of the supplemental material indicate that the effect of suppressing strong correlations is to recover a linear relation between the total node weights and their degrees.

Given Ceará state's vast area, alongside its uneven wealth distribution and diverse population density patterns, our approach is twofold. First, we aim to identify clusters of cities by examining the intensity of their mutual trades. Subsequently, we will assess how closely their economic interests align with what we term as community "cohesiveness". For

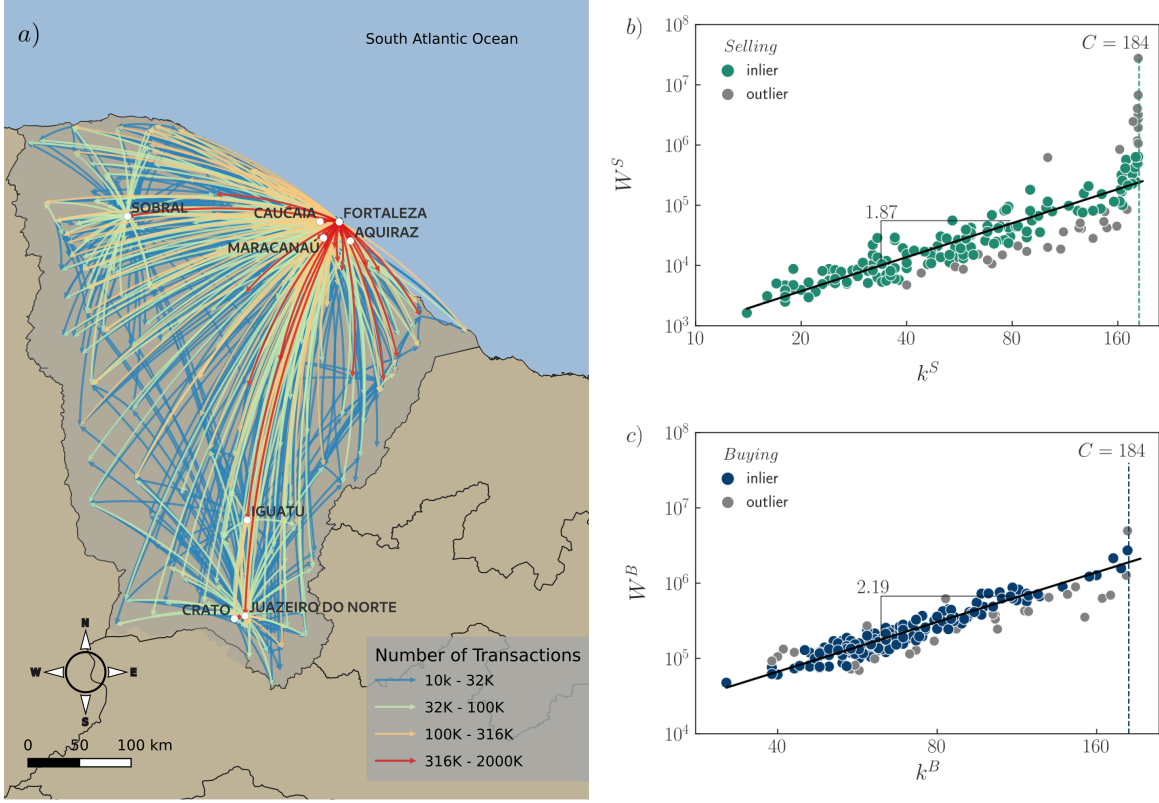


FIG. 1. a) The trade network among municipalities superimposed on the map of the Ceará state, Brazil. The nodes are located at the geographic position of each city. The color of each edge is coded according to the number of transactions between a pair of nodes, from blue to red, corresponding to low and high values, respectively, and its direction is from the city that sells to the city that buys the products. Only edges with more than 10000 transactions are displayed. b) Scaling relation between the total number of internal sales transactions (out-transactions), W^S , and the total number of internal sales connections (out-degree), k^S , both computed for all cities in the state of Ceará from a database comprising approximately 3.7 billion records of electronic invoices registered during the period from 2016 to 2019. Green and gray circles correspond to the inlier and outlier data points, respectively, and the continuous green line represents the best fit to a power-law, $W^S \simeq (k^S)^\beta$, with the exponent $\beta = 1.87 \pm 0.03$, 95% confidence interval and $R^2 = 0.89$. c) The same as in (b), but for the total number of internal buying transactions (in-transactions), W^B , and the total number of internal buying connections (in-degree), k^B . Blue and gray circles correspond to the inlier and outlier data points, respectively, and the continuous blue line represents the best fit to a power-law, $W^B \simeq (k^B)^\beta$, with the exponent $\beta = 2.19 \pm 0.01$, 95% confidence interval and $R^2 = 0.94$.

the initial task, we have chosen the Infomap algorithm, [45–47] since it is compatible with the most relevant and inherent feature of the system under investigation here, namely, a network of flows, in particular, flows of financial resources based on trade operations among cities. Accordingly, this flow-based algorithm makes use of an information-theoretic method to detect network communities with a very high computational performance. Figure 2a shows the map of the Ceará state in Brazil colored according to the communities detected via the Infomap algorithm. The algorithm identifies a partition with the minimal average per-step description length of the random walk. Interestingly, the two-dimensional geographical projections of the resulting five modules clearly show that they are all *simply-connected domains*, *i.e.*, well-delimited single pieces without holes [48, 49]. This result demonstrates the consistency and corroborates the adequacy of the flow-based algorithm, which is in evident contrast with other approaches relying on pairwise interactions and the network formation process, as it is the case, for example, with the generalized modularity [50]. For a comparison, we show in with Fig. 2b the communities detected using the stochastic block model [18]. Clearly, the large number of communities, their heterogeneity in space, and lack of contiguity among their constituting pieces indicate that the method is unable to capture the economic dynamics embedded in the trade network of sales and buying among cities.

In Fig. 3 we show the trade share matrix after clustering the municipalities using the Infomap, with the communities delimited by black continuous lines. The matrix has color-coded entries according to the number of transactions between a pair of nodes, from blue to red, corresponding to low and high values, respectively. Moreover, it is non-symmetrical, with rows reaching the cities that sell to the ones buying in the columns. In each community, we highlighted the leading cities in terms of population and monetary resources. These cities, including Fortaleza, the capital of Ceará, present a wide spectrum transactions that virtually extends to all other cities in the state.

III. COMMUNITY DETECTION

Having studied the topological properties of the networks of transactions, we next analyze the database of electronic invoices from the perspective of the traded products. To this end, we build bipartite networks, one for selling and another for buying, in which the two types of nodes are the cities of Ceará state and the products they trade, sell or buy, respectively, with

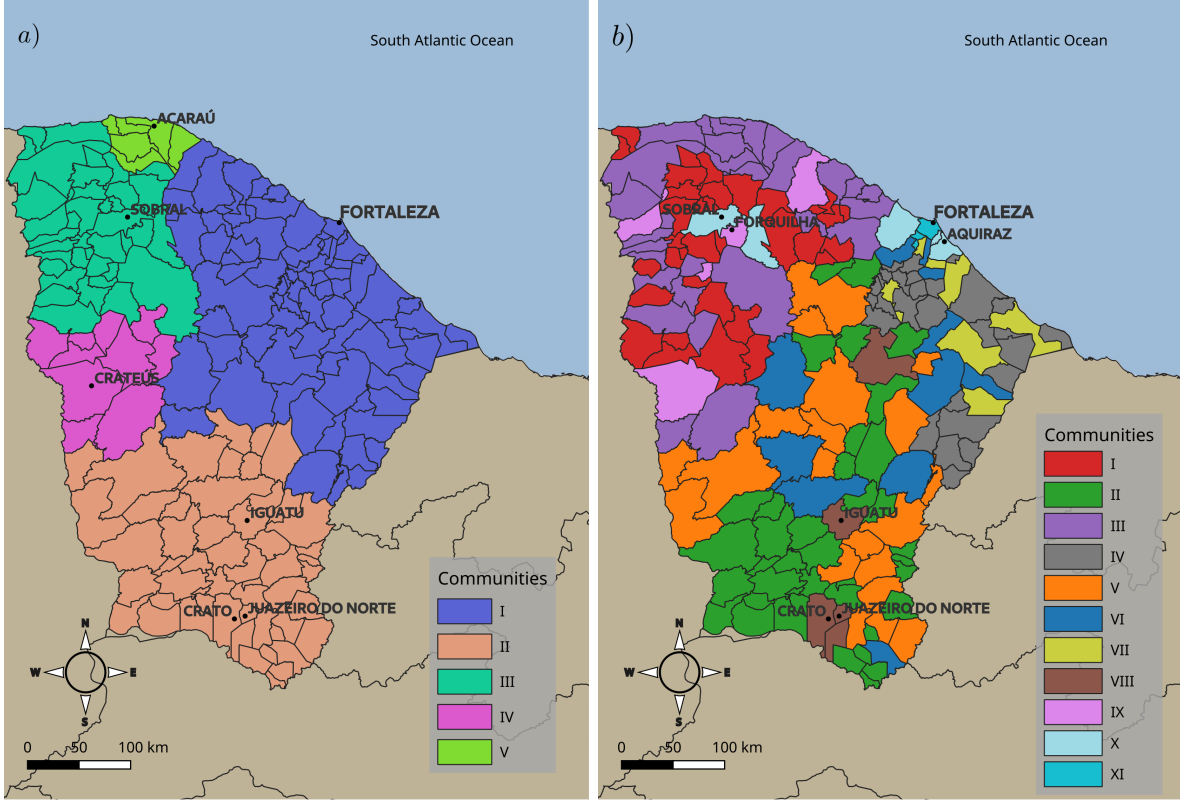


FIG. 2. Shown in (a) is the map of the Ceará state in Brazil colored according to the communities detected via the Infomap algorithm [45], which identifies the partition M that provides the shortest description length and captures the optimal community structure of the network of commercial transactions between cities in terms of its associated flow dynamics. As a noteworthy result, the algorithm is capable to identify a partition with five modules, whose two-dimensional geographical projections are all simply-connected domains, *i.e.*, consisting of single pieces without holes. Highlighted are the leading seven cities in each community in terms of population and monetary resources. The results shown in (a) points to the reliability and validates the effectiveness of the flow-based Infomap algorithm [45], which strongly contrasts with alternative methods for modularity detection basically relying on pairwise interactions and features of the network formation process, as it is the case with generalized modularity techniques [41]. For comparison, the communities identified using the stochastic block model [18] are shown in (b).

any other city in the country. Following [10], the products are identified in the electronic invoices using the HS [11, 12]. The presence of a link in these networks should reflect the relative importance of the selling or buying transactions of a given city c involving the product p in a balanced context of all transactions among all cities and all products traded in the

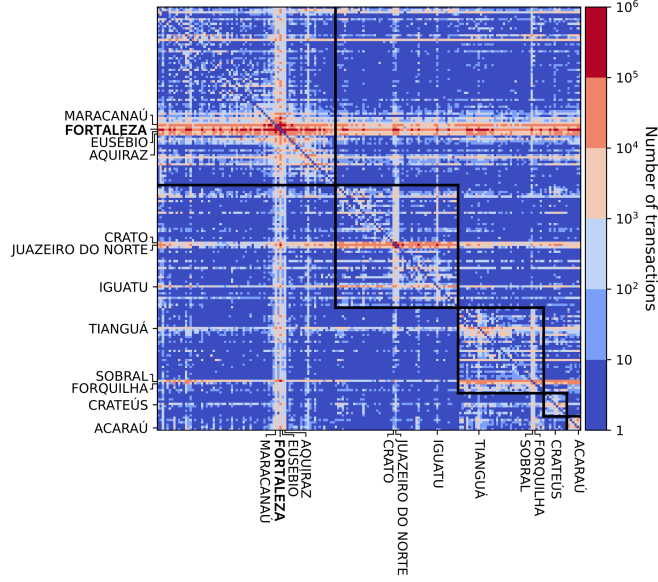


FIG. 3. The trade share matrix after clustering between municipalities. We sorted the cities according to the optimal partition found using the Infomap algorithm and highlighted the leading cities in terms of their number of transactions. The communities are separated by the solid black lines. The matrix has entries color-coded according to the number of transactions between a pair of cities, from blue to red, corresponding to low and high values, respectively. It is important to note the far-reaching strong connections of the highlighted cities.

system. This is achieved here by adopting the concept of Revealed Comparative Advantage (RCA) index [6], quantified in terms of the complexity of products and the diversification of the cities' baskets of traded products. More precisely, in order to determine the relevant transactions, we adopt the following model of activation of products: let $q_{c,p}^S$ be the monetary value associated with a city c selling a product p to a different municipality in the state of Ceará or any other city in Brazil. Thus $T_c^S = \sum_p^P q_{c,p}^S$ corresponds to the total sales of the city c , the summation running over all P products traded in the state. On the other hand, the amount $T_p^S = \sum_c^C q_{c,p}^S$ adds up to the total sales of a product p , the summation now running over all C municipalities in the state of Ceará. Likewise, the quantity $T_{tot}^S = \sum_{c,p}^{C,P} q_{c,p}^S$ amounts to the total monetary value associated with the sales of all products P by all cities C in the state during the investigated time window. From these three quantities, we can compute the quotient of quotients,

$$Q_{c,p}^S = \frac{q_{c,p}^S/T_c^S}{T_p^S/T_{tot}^S}, \quad (1)$$

where the numerator corresponds to the relative value of the sales of product p by city c , compared to all sales of this city. The denominator is the relative of value of all sales of the product p to all sales of the state. Equation (1) is the usual definition of an element of the RCA matrix [6, 7, 51] which we are here extending to the trades among municipalities. If $Q_{c,p}^S > 1$, it means that product p is relatively more important to the sales of city c than the relative importance of all sales of this product by all cities. In this case, we say that the municipality c is a “seller” of product p . We apply the same reasoning for $Q_{c,p}^B$ representing the monetary value associated with the purchases of product p by the municipality c . In this case, if $Q_{c,p}^B > 1$, it means that buying product p is relatively more important to the city c than the relative importance of all purchases of this product by all cities of the state, so that the municipality c is a “buyer” of product p .

From the RCA matrix for sales, \mathbf{Q}^S , obtained using Eq. (1), we can construct the corresponding binarized municipality-product matrices $\boldsymbol{\sigma}^S$, with the *activity* elements defined by

$$\sigma_{c,p}^S = \begin{cases} 1, & \text{if } Q_{c,p}^S \geq 1 \\ -1, & \text{if } Q_{c,p}^S < 1, \end{cases} \quad (2)$$

for each city $c = 1, 2, 3, \dots, C$ and product $p = 1, 2, 3, \dots, P$. The same transformation is applied to the RCA matrix for buying, \mathbf{Q}^B , so that the binary matrix $\boldsymbol{\sigma}^B$ with activities elements $\sigma_{c,p}^B$ can also be obtained. The *diversity* of the basket of products for sales of a given city c , defined as $D_c^S = \sum_p^P (\sigma_{c,p}^S + 1)/2$, corresponds to the number of relevant products the city sells, while the *ubiquity* for sales of a given product p , defined as $U_p^S = \sum_c^C (\sigma_{c,p}^S + 1)/2$, corresponds to the number of cities whose baskets of relevant products for sales include the product p . In the same fashion, the diversity of the basket for buying of a city c , D_c^B , and the ubiquity for buying of a product p , U_p^B , can be readily obtained from the elements of the binary matrix $\boldsymbol{\sigma}^B$. Figure 4 shows the raster plots of the municipality-product matrices $\boldsymbol{\sigma}^B$ and $\boldsymbol{\sigma}^S$, with the cities sorted in the descending order in terms of their respective diversity (from top to bottom), and the products sorted in the descending order (from left to right) in terms of their respective ubiquity. Upon examination, the municipality-product matrix for buying transactions (Fig.4a) is markedly denser than the one for selling transactions (Fig.4b). This observation is straightforward to grasp. First notice that both matrices share the same set of municipalities and the same product basket. The observed asymmetry reveals the diversification of consumption behaviors. Specifically, municipalities and their

inhabitants engage in purchasing a wide range of products, many of which are not produced locally. On the other hand, production trends are far more specialized. Municipalities tend to focus on manufacturing specific products, influenced by factors such as the availability of resources, specialized expertise, labor considerations, and historical contexts. When focussing on commerce, economies of scale become evident. For some products, distribution is more efficient when undertaken by a small number of municipalities dealing in significant volumes. Such disparities in transactional behaviors are responsible for the observed asymmetry. For the case in study, the most frequent classes of products are “Appliances for Agriculture”, “Rice Cultivation” and “Mineral Fuels” for buying, while “Building Bricks”, “Mineral Water”, and “Fruit and Vegetable Conserves” are the most frequent classes for selling. The cities of Fortaleza, Juazeiro do Norte, Maracanaú, Quixadá, and Eusébio are the cities with the most diverse baskets of products for selling transactions, while Fortaleza, Juazeiro do Norte, Maracanaú, Sobral, and Caucaia have the higher diversities in the case of buying.

IV. MAXIMUM ENTROPY MODEL

In this study we aim to investigate the statistics of product activities of the cities from the perspective of a pairwise Maximum Entropy Model. We follow the approach proposed in Refs. [21, 32, 33, 52–55] to build an Ising-like model for a given community, which is capable of replicating the average activities and pairwise correlations in terms of the product baskets for each city in this community. We then evaluate the behavior of the resulting model in the analogous framework of the corresponding thermal equilibrium properties. Accordingly, for a given community, from the observed product series of the activity of a city i , as defined in Eq. (2), we can calculate its product-average activity as,

$$\langle \sigma_i \rangle^{obs} = \frac{1}{P} \sum_{p=1}^P \sigma_{i,p}, \quad (3)$$

as well as the covariances between the product series of the activities (for selling or buying) of each pair of cities i and j ,

$$Cov_{ij}^{obs} = \langle \sigma_i \sigma_j \rangle^{obs} - \langle \sigma_i \rangle^{obs} \langle \sigma_j \rangle^{obs}, \quad (4)$$

where $\langle \sigma_i \sigma_j \rangle^{obs} = \frac{1}{P} \sum_{p=1}^P \sigma_{i,p} \sigma_{j,p}$. Moreover, to model the observed activities, we consider that σ correspond to Ising-like variables on a fully connected network of C sites. Therefore, in analogy with Statistical Mechanics, $\{\sigma\} = \{\sigma_{1,p}, \dots, \sigma_{C,p}\}$ would be descriptive

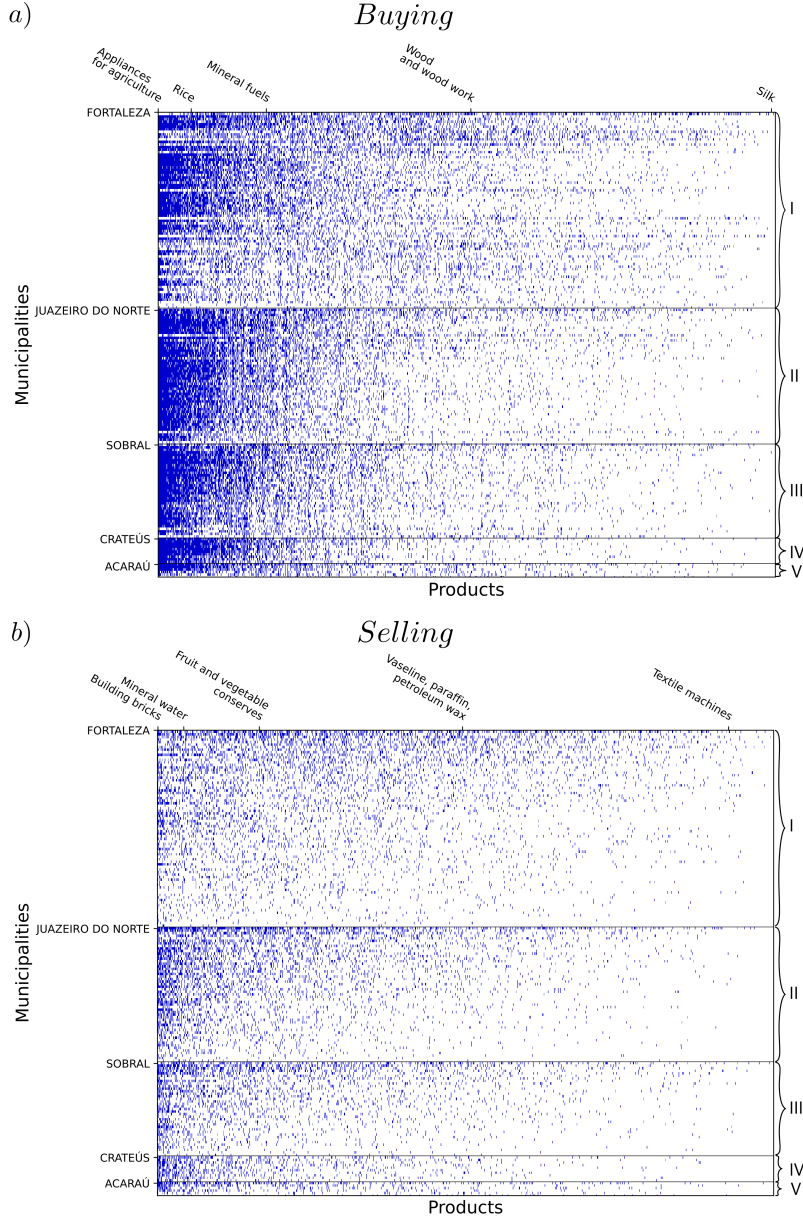


FIG. 4. Raster plots of the municipality-product matrices for buying σ^B (a) and selling σ^S (b). The rows are sorted in the descending order of the diversity, $D_c^S = \sum_p \sigma_{c,p}^S$, for cities (from top to bottom) in each community, and the columns in the descending order of the ubiquity, $U_p^S = \sum_c \sigma_{c,p}^S$, for the products (from left to right). Accordingly, for each municipality c , the state $\sigma_{c,p}^S$ for the sales of a product is active (+1) if $Q_{c,p}^S \geq 1$ (blue) or inactive (-1) if $Q_{c,p}^S < 1$ (white). The same rule is used for the purchase of a product, $\sigma_{c,p}^B$. Highlighted are the leading cities of each community in terms of diversity and the most ubiquitous products. The products are identified by using a code in the electronic invoices that follows the HS [11, 12].

of “the configuration of the community” with respect to a given product p . The probability distribution $P(\{\sigma\})$ that represents our system is the one that maximizes the entropy, $S = -\sum_{\{\sigma\}} P(\{\sigma\}) \ln P(\{\sigma\})$, while reproducing our observations, *i.e.*, $\langle \sigma_i \rangle^{obs}$ for all C cities and all $C(C-1)/2$ values of Cov_{ij}^{obs} . Given these two additional constraints, it can be readily shown [53] that the form of $P(\{\sigma\})$ is the Boltzmann’s probability distribution for a temperature $T = T_0 = 1$,

$$P(\{\sigma\}) = \frac{1}{Z} e^{-\mathcal{H}(\{\sigma\})/T}, \quad (5)$$

where $Z = \sum_{\{\sigma\}} e^{-\mathcal{H}(\{\sigma\})/T}$ is the partition function and \mathcal{H} is analogous to a Hamiltonian with the same form of the Ising model,

$$\mathcal{H}(\{\sigma\}) = -\sum_{i=1}^C h_i \sigma_i - \sum_{i,j>i}^C J_{ij} \sigma_i \sigma_j. \quad (6)$$

It should be noted that this model is derived directly from empirical data through the maximum entropy principle, rather than being presumed as a simplified representation of the underlying dynamics. As such, this method constitutes a precise mapping and not merely a figurative comparison. Equations (5) and (6) together are designed to calculate, based on the observed inter-city correlations, the likelihood of all possible states across the entire network of cities. This represents a baseline model, implying that the actual network might exhibit greater complexity than what the maximum entropy model indicates, but certainly not less.

This Ising-like correspondence naturally leads us to interpret h_i as the action of a local external stimulus on the product activity of the city i , analogous to a “random field”, and J_{ij} as a “coupling coefficient” between cities i and j . Such pairwise couplings or interactions between the product activities of cities give rise to the observed correlations between them. At this point, we compute the local fields h_i and the interactions J_{ij} by directly solving the inverse problem given by Eq. (6). The local fields h_i and interaction constants J_{ij} are obtained through the following iterative scheme:

$$J_{ij}(n+1) = J_{ij}(n) - \eta(n) [Cov_{ij}^{MC} - Cov_{ij}^{obs}], \quad (7)$$

$$h_i(n+1) = h_i(n) - \eta(n) [\langle \sigma_i \rangle^{MC} - \langle \sigma_i \rangle^{obs}], \quad (8)$$

where n is the iteration parameter and we start with $n = 1$ and $h_i(n = 1) = 0$. The covariance Cov_{ij}^{MC} between two sites i and j of the Ising-like network of Eq. (6) is given by $Cov_{ij}^{MC} = \langle \sigma_i \sigma_j \rangle^{MC} - \langle \sigma_i \rangle^{MC} \langle \sigma_j \rangle^{MC}$, where the statistical average $\langle \dots \rangle^{MC}$ is obtained by

performing a Monte Carlo simulation of the model Eq. (6) at temperature $T_0 = 1$ using $h_i(n)$ and $J_{ij}(n)$. The function $\eta(n)$ is a learning rate which decays like $1/n^{0.4}$ [56]. Typically, we iterate till $n = 80000$. Once we infer the values of h_i and J_{ij} that better reproduce the observed product-average activities $\langle \sigma_i \rangle^{obs}$ and covariances Cov_{ij}^{obs} , while maximizing the entropy, the Boltzmann probability distribution of Eq. (5) characterizes the statistics of the product activities of the cities composing a given community dataset.

By solving Eqs. (7) and (8) simultaneously, we obtain for each community and for both buying and selling cases, their corresponding local fields h_i and coupling constants J_{ij} . As shown in Fig. 5, the distributions of the fields h_i indicate that they are predominantly negative, with those for selling transactions being systematically more negatively skewed than those for buying. Comparatively, as shown in Fig. 6, the distributions of the coupling interaction constants J_{ij} are symmetrically centered around zero. Additionally, for all three communities they can be accurately characterized as Gaussian's with mean values close to zero, but with standard deviations that are systematically smaller for buying operations than for selling.

To assess the efficacy of the Ising-like model described by Eq. (6) in replicating measured averages derived from observational data, we compare in Fig. 7 the final product-averaged magnetizations obtained from the MEM, $\langle \sigma_i \rangle^{MC}$, with their observational counterparts, $\langle \sigma_i \rangle^{obs}$, for each city i within the three largest communities labeled I, II, and III, respectively. The same is shown in Fig. 8, but for the covariances Cov_{ij}^{MC} against Cov_{ij}^{obs} between every pair of cities i and j in the aforementioned communities. Clearly, the concordance between the model-generated and observational metrics is excellent across all examined cases. To provide a more conclusive test of the model, we compared the three-point activity correlations generated by the model, T_{ijk}^{MC} , with those observed, T_{ijk}^{obs} , where $T_{ijk} = \langle (\sigma_i - \langle \sigma_i \rangle) (\sigma_j - \langle \sigma_j \rangle) (\sigma_k - \langle \sigma_k \rangle) \rangle$. As depicted in Fig. 9, both the model's predictions and the observed triplet correlations exhibit a strong correlation across all cases, that is, for both the buying and selling scenarios in the three communities. Moreover, the quantitative alignment between them is also quite satisfactory, with relative errors, $\langle (T_{ijk}^{MC} - T_{ijk}^{obs}) / T_{ijk}^{obs} \rangle$, of $-0.33\% \times 10^{-3}$, -0.093% , and 0.12% for the buying scenarios, and -0.54% , 0.004% , and -0.062% for the selling scenarios, in relation to Communities I, II, and III, respectively.

After demonstrating that the Ising-like model adequately represents the product-averaged properties of the three largest communities in both selling and buying scenarios, we explore

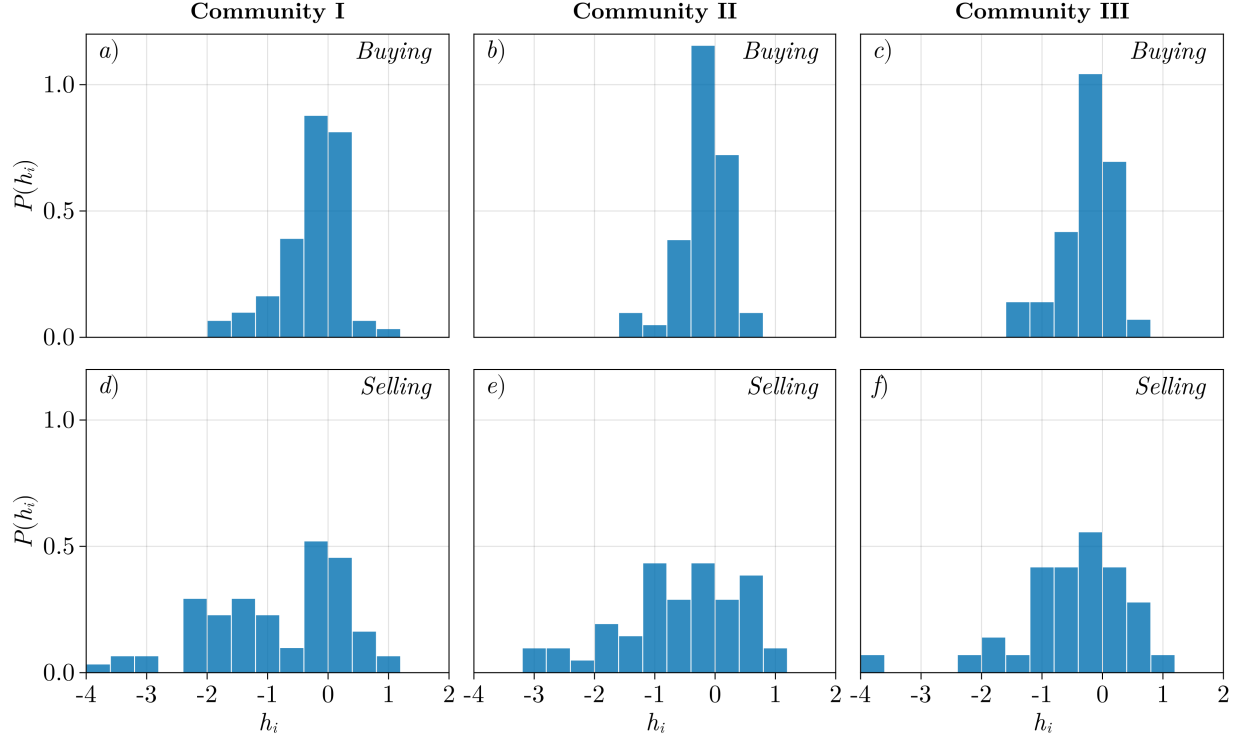


FIG. 5. Distribution of local fields h_i after learning. The figures *a)*, *b)*, and *c)* illustrate the distributions for *selling* transactions in Communities I, II, and III, respectively, while figures *d)*, *e)*, and *f)* depict the distributions for *buying* transactions in Communities I, II, and III, respectively. It's observed that all distributions show negative skewness γ_1 , indicating a predominance of smaller values. The specific values of γ_1 for each graph are: *a)*: $\gamma_1 = -0.90$; *b)*: $\gamma_1 = -0.94$; *c)*: $\gamma_1 = -0.80$; *d)*: $\gamma_1 = -0.52$; *e)*: $\gamma_1 = -0.63$; *f)*: $\gamma_1 = -1.23$.

deeper into the implicit thermodynamic analogy introduced by the MEM methodology [53]. Within this framework, using the learned J_{ij} and h_i parameters along with Eqs. (5) and (6), we conduct Monte Carlo simulations at temperatures T other than the operational temperature $T_0 = 1$. Given the magnetization for each configuration, defined as $M(\{\sigma\}) = \left| \frac{1}{C} \sum_i^C \sigma_i \right|$, the order parameter for a ferromagnetic phase transition can be represented by the ensemble average at a constant temperature T . This is mathematically expressed as:

$$M(T) = \langle M(\{\sigma\}) \rangle_T^{MC}. \quad (9)$$

In this equation, the statistical average $\langle \dots \rangle_T^{MC}$ is calculated using Monte Carlo simulations at temperature T . Additionally, considering the energy per city for each configuration as

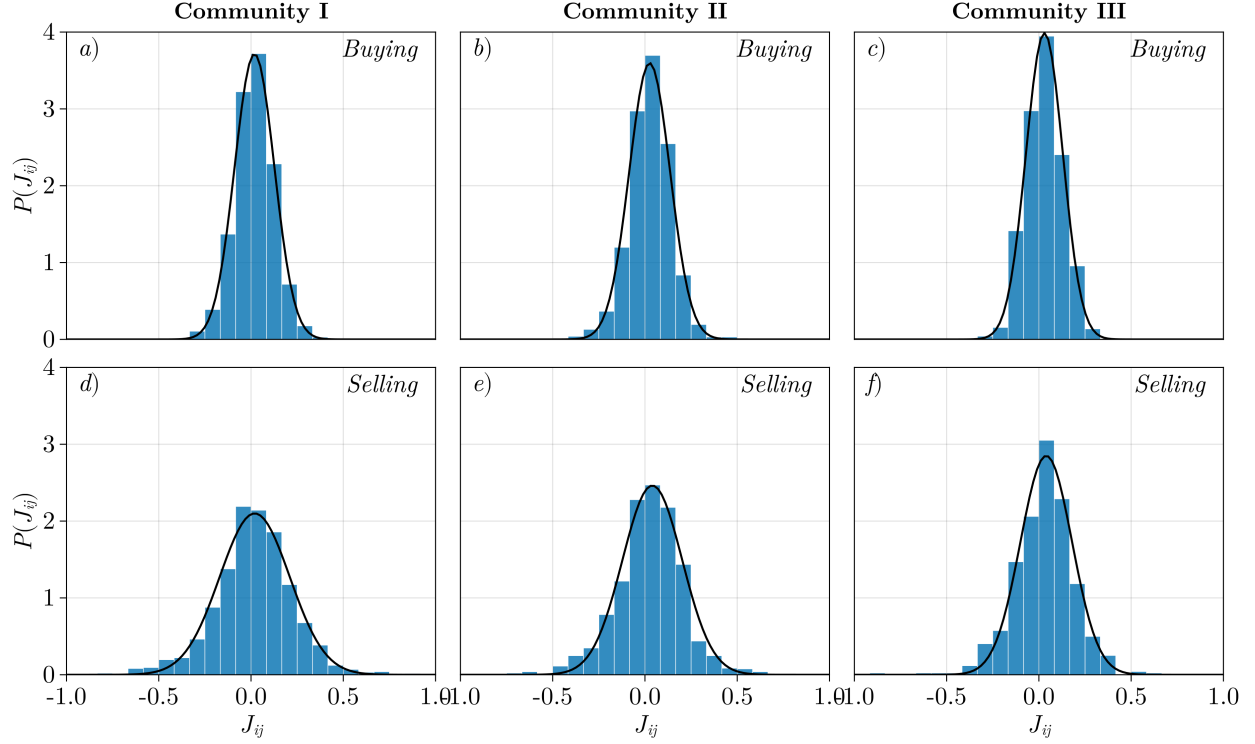


FIG. 6. Distributions of couplings J_{ij} . Shown in a), b), and c) are the distributions for *selling* transactions and in figures d), e), and f) are the distributions for *buying* transactions in Communities I, II, and III, respectively. The data were fitted to Gaussian distributions, and the adequacy of this model was confirmed by the Kolmogorov-Smirnov (KS) test, yielding a p-value > 0.05 in all cases. This result suggests a satisfactory agreement between the observed data and the Gaussian model. The fitting parameters (mean μ and standard deviation σ) and their respective p-values are: a): $\mu = 0.02$, $\sigma = 0.11$, p-value = 0.28; b): $\mu = 0.03$, $\sigma = 0.12$, p-value = 0.21; c): $\mu = 0.03$, $\sigma = 0.10$, p-value = 0.96; d): $\mu = 0.02$, $\sigma = 0.19$, p-value = 0.08; e): $\mu = 0.04$, $\sigma = 0.16$, p-value = 0.10; f): $\mu = 0.04$, $\sigma = 0.15$, p-value = 0.23;

$E(\{\sigma\}) = \frac{1}{C} \mathcal{H}(\{\sigma\})$, the fluctuation-dissipation theorem leads to the following expression for the specific heat:

$$C(T) = \frac{1}{T^2} (\langle E(\{\sigma\})^2 \rangle - \langle E(\{\sigma\}) \rangle^2). \quad (10)$$

In Fig. ??a and ??b of the supplemental material, we present the average magnetization $M(T)$ as a function of temperature T for the buying and selling activities of the three largest communities, respectively. The magnetization starts to rapidly decrease near the temperature

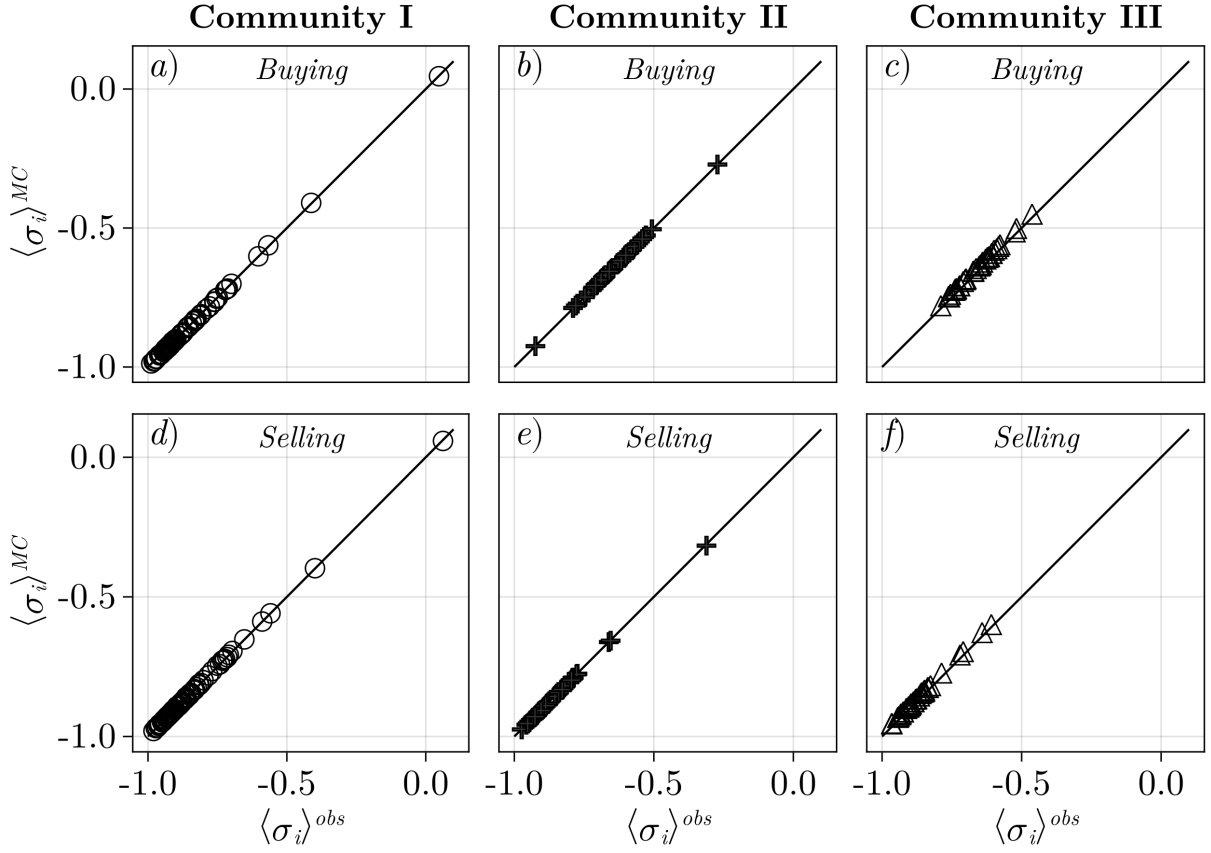


FIG. 7. Comparison between the observed average magnetizations, $\langle \sigma_i \rangle^{obs}$, and those predicted by the Maximum Entropy Model via Monte Carlo simulations, $\langle \sigma_i \rangle^{MC}$. Panels a), b), and c) display results corresponding to the average selling activities, while panels d), e), and f) pertain to buying activities. Each set of three panels represents Communities I, II, and III, respectively. The excellent agreement observed across all cases highlights the effectiveness of the method in terms of the converged parameters h_i and J_{ij} constituting the Ising-like model, as described in Eq. (6).

$T = 1.0$, indicating a change in behavior that is analogous to a phase transition from ordered to disordered spin configurations with critical temperatures T_c that, for all cases, are close to the operational temperature T_0 . The macroscopic ordering diminishes for all analyzed communities as the temperature ascends. Notably, at temperatures significantly above the critical ones, the magnetizations observed for the selling curves of all three communities saturate at larger values compared to the buying cases. This behavior can be attributed to the local fields distributions showcasing a pronounced skewness toward negative values in the selling scenario, as shown in Fig. 5, thereby mitigating the extent of its order-disorder

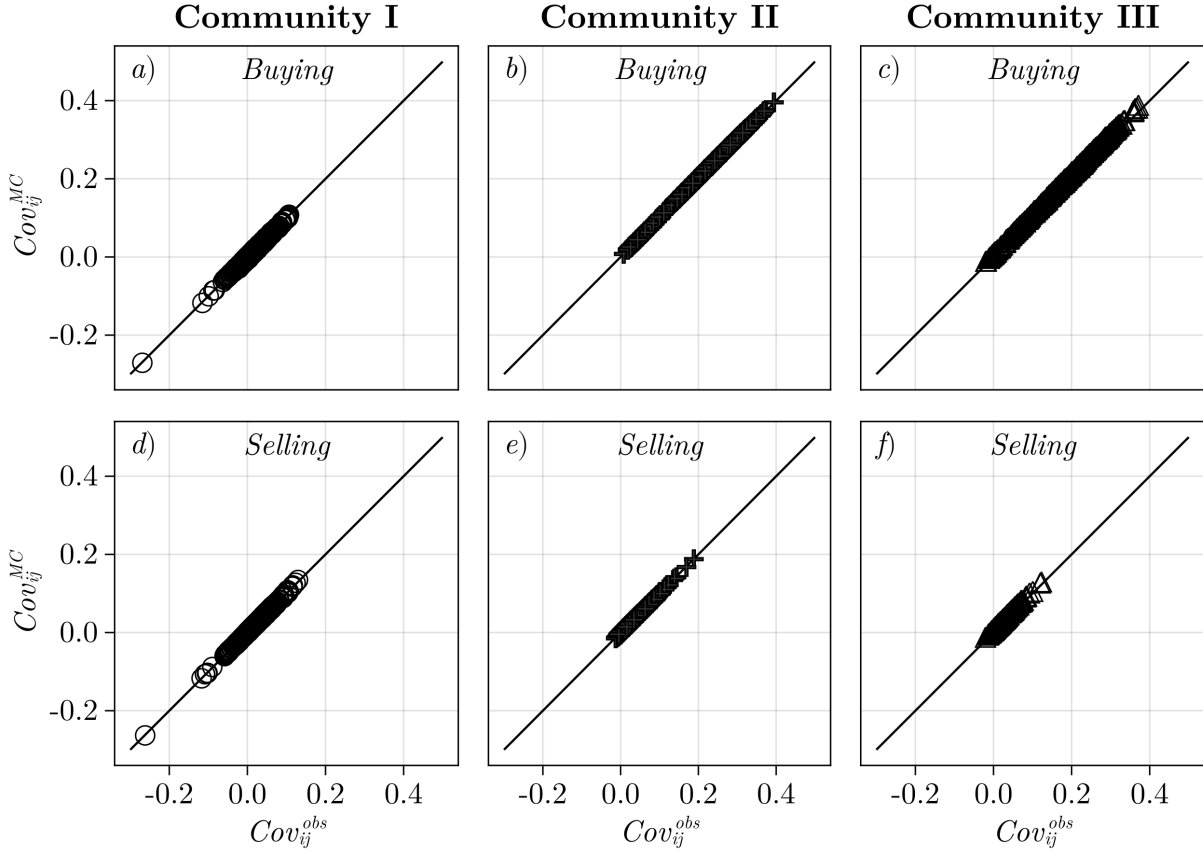


FIG. 8. Comparison between observed covariances, Cov_{ij}^{obs} , and those predicted by the MEM through Monte Carlo simulations, Cov_{ij}^{MC} . The results in a), b), and c) correspond to selling average activities, while those in d), e), and f) are for buying, with the three panels in both sets referring to Communities I, II, and III, respectively. The excellent agreement in all cases reflects the convergence of the method in terms of the parameters h_i and J_{ij} constituting the Ising-like model Eq. (6).

transition.

Figures 10a and 10b depict the temperature-dependent specific heat, $C(T)$, computed for the three largest communities in relation to their buying and selling product baskets, respectively. In both scenarios, each curve peaks at a temperature T_c , which, while exceeding the operating temperature $T_0 = 1$, remains in close proximity to it (refer to Table I for specific numerical values). Given this observation, it is reasonable to assert that the learning dynamics of the six Boltzmann machines predominantly take place within the “critical region”. This “critical temperature” T_c serves as a threshold, distinguishing the ordered phases (for

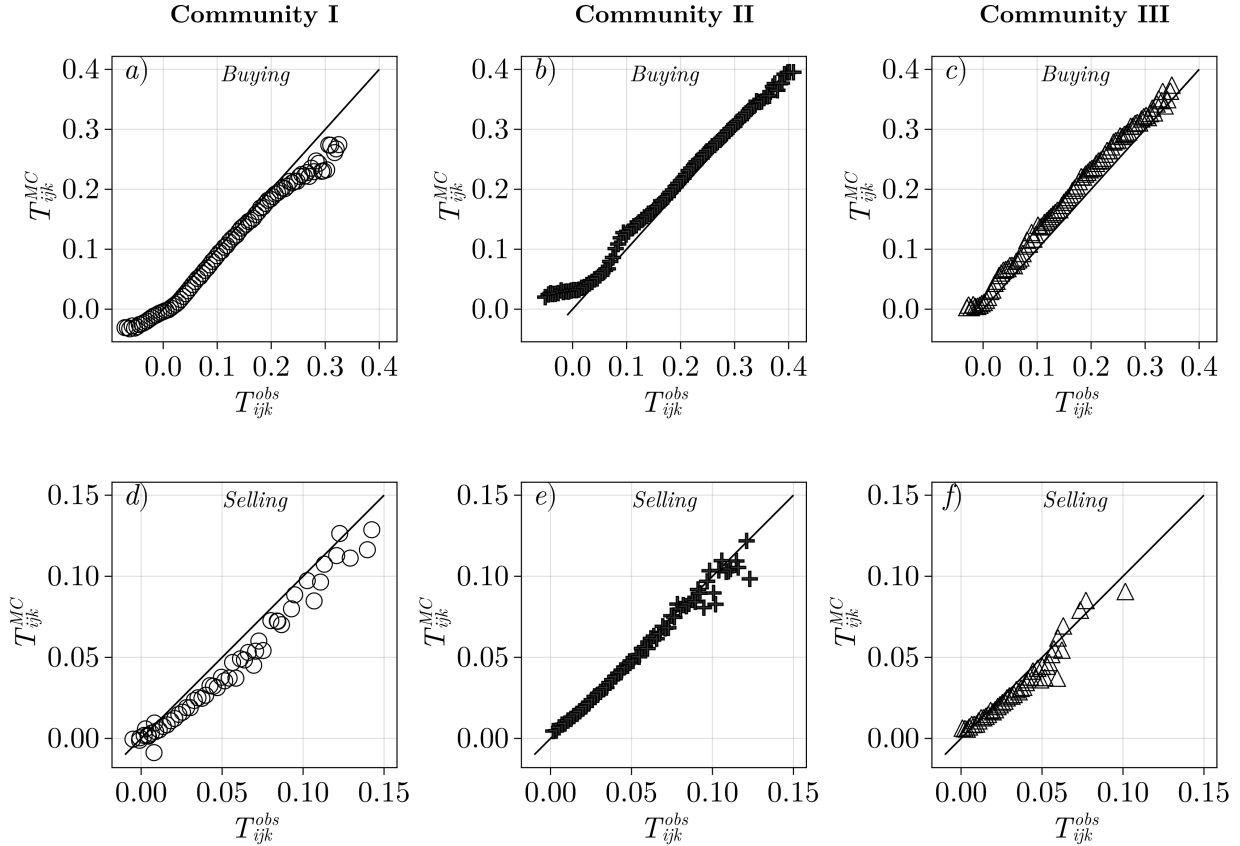


FIG. 9. Comparison of three-point spin correlations as generated by the model, T_{ijk}^{MC} , and as observed, T_{ijk}^{obs} . Clearly, the model’s predictions and the observed triplet correlations exhibit a strong correlation in both the buying and selling scenarios across all three communities. Furthermore, the quantitative alignment between them is also quite satisfactory. The relative errors are equal to -0.003 , -0.001 , and 0.001 for the buying scenarios and -0.005 , 0.000 , and -0.001 for the selling scenarios, in relation to Communities I, II, and III, respectively.

$T < T_c$) from the disordered phases (for $T > T_c$). A comparison between Figs. 10a and 10b indicates that the energy fluctuations for buying are more pronounced than for selling. Also shown in Figs. 10a and 10b is the dependence of the specific heat on temperature, obtained after randomly shuffling the product series associated with the buying and selling activities of Community I, respectively. This random shuffling can significantly reduce the intrinsic correlations present in the sequence of “spins”. Notably, under these conditions, the pronounced peak in the specific heat becomes significantly subdued, effectively undermining the ferromagnetic phase transition originally observed in the system.

TABLE I. $(T_0 - T_c)$ for different communities and transaction type.

	I	II	II	I-shuffled
Selling	0.09	-0.02	-0.01	0.49
Buying	-0.05	-0.06	-0.1	0.49

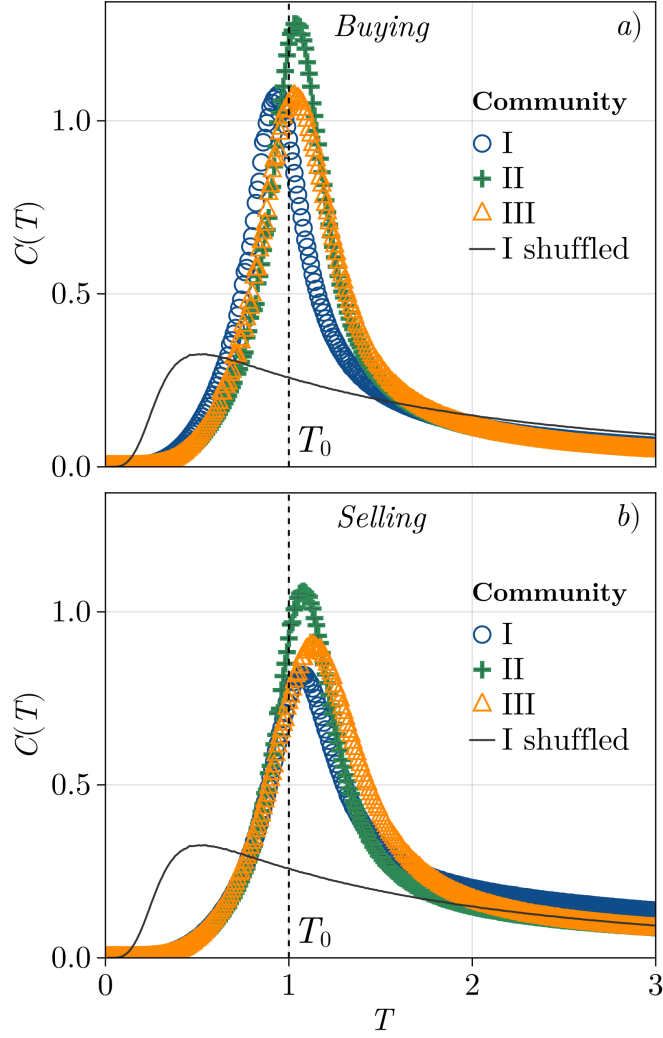


FIG. 10. Specific heat $C(T)$ as a function of the temperature T for the three largest communities of cities in the state. All curves exhibit maximal values, C^* , at given “critical temperatures”, T^* , that are above, but quite close to the operating temperature $T_0 = 1$. In the case of buying, as shown in *a*), the peak of the heat capacity becomes closer to the operating point as the size of the community decreases. In the case of selling, as shown in *b*), the larger the community, shorter is its corresponding distance to the “critical point”. In both buying and selling cases, however, the maximum value C^* increases with system size.

V. CONCLUSIONS

In summary, we have shown that the directed-weighted trade network among the municipalities exhibits a nontrivial dependence between the weights of the nodes on their degrees. From the least-squares fit of the sales inlier data to the power law, $W^S \sim (k^S)^\beta$, we obtained $\beta = 2.07 \pm 0.01$, while the fitting of the purchasing inlier data to $W^B \sim (k^B)^\beta$, resulted in $\beta = 1.77 \pm 0.02$.

In the topological analysis, the use of the Infomap algorithm has revealed five communities within the trade network among municipalities. Strikingly, the two-dimensional geographical projections of these modules clearly show that they are all simply-connected domains. This reflects that the trade network is inherently characterized by the flow of products. This finding highlights the lasting significance of geographic proximity in shaping trade patterns, even in the era of globalized economies. Such contiguous trade communities, identified purely based on trade flow data, suggest that regional economic interactions are strongly influenced by spatial factors. This has significant implications for regional economic policy, emphasizing the potential for more targeted and regionally coherent economic strategies. For comparison, during the writing of this paper, the Ceará state has 14 administrative macro-regions that were established by extensive studies taking into account technical criteria related to natural resources, social solidarity, and polarization around urban centers [57]. The contrast between these findings and the results from other algorithms like the stochastic block model not only reinforces the uniqueness of Infomap’s approach in capturing the flow-based nature of trade but also points to the nuanced complexities inherent in trade network analysis. This understanding can guide future policy decisions and economic planning, emphasizing the relevance of local and regional contexts in economic networks.

Finally, conceptualizing cities and their trading patterns in terms of buying and selling products as spin systems has enabled us to harness well-developed theories from physics to interpret complex economic behaviors. Specifically, for the purchasing trade operations, we employed a Boltzmann machine that uses a Hamiltonian analogous to that of a Spin-Glass model, which maximizes the system’s entropy subject to the observed “magnetizations” and “spin-spin correlations”. Our findings indicate that the system operates very close to a critical point, poised for a phase transition from ordered states (“ferromagnetic”), where cities exhibit clustered buying behaviors, to disordered states (“paramagnetic”), where the decision to buy

a given product appears random. The same analyzes is applicable to selling operations. Being close to a critical point is particularly revealing, since they are hallmarked by scale-invariant fluctuations, suggesting that our economic system is on the verge of a shift, highly sensitive to both external and internal disruptions. Furthermore, this proximity to a critical point implies that minor changes in a single city’s economic strategy (or product purchases) could ripple through and potentially catalyze large-scale alterations in the broader economic landscape. Such a dynamic signifies a marketplace characterized by rich, interconnected activities with an inherent potential for rapid evolution. These insights could have profound implications for understanding the resilience and adaptability of economies as well as for informing strategic economic policies.

VI. ACKNOWLEDGEMENTS

We thank the Brazilian agencies CNPq, CAPES, FUNCAP and the National Institute of Science and Technology for Complex Systems (INCT-SC) for financial support.

-
- [1] Ceará | Cidades e Estados | IBGE (2023), accessed 2023-09-02.
 - [2] C. A. Hidalgo and R. Hausmann, The building blocks of economic complexity, *Proc. Natl. Acad. Sci. U. S. A.* **106**, 10570 (2009).
 - [3] C. A. Hidalgo, Economic complexity theory and applications, *Nat. Rev. Phys.* **3**, 92 (2021).
 - [4] A. Tacchella, M. Cristelli, G. Caldarelli, A. Gabrielli, and L. Pietronero, A new metrics for countries’ fitness and products’ complexity, *Sci. Rep.* **2**, 723 (2012).
 - [5] A. Tacchella, M. Cristelli, G. Caldarelli, A. Gabrielli, and L. Pietronero, Economic complexity: Conceptual grounding of a new metrics for global competitiveness, *J. Econ. Dynam. Control* **37**, 1683 (2013).
 - [6] C. A. Hidalgo, B. Klinger, A.-L. Barabasi, and R. Hausmann, The product space conditions the development of nations, *Science* **317**, 482 (2007).
 - [7] B. Balassa, Trade liberalisation and “revealed” comparative advantage, *Manchester Sch.* **33**, 99 (1965).

- [8] P.-A. Balland, T. Broekel, D. Diodato, E. Giuliani, R. Hausmann, N. O’Clery, and D. Rigby, The new paradigm of economic complexity, *Res. Pol.* **51**, 104450 (2022).
- [9] C. D. Brummitt, A. Gómez-Liévano, R. Hausmann, and M. H. Bonds, Machine-learned patterns suggest that diversification drives economic development, *J. R. Soc. Interface* **17**, 20190283 (2020).
- [10] G. Alhora, L. Pietronero, A. Tacchella, and A. Zaccaria, Product progression: a machine learning approach to forecasting industrial upgrading, *Sci. Rep.* **13**, 1421 (2023).
- [11] H. Asakura, The harmonized system and rules of origin, *J. World Trade* **27**, 5 (1993).
- [12] W. C. Organization, *Hs nomenclature 2017 edition* (2017), accessed 2023-05-12.
- [13] N. Jean, M. Burke, M. Xie, W. M. Davis, D. B. Lobell, and S. Ermon, Combining satellite imagery and machine learning to predict poverty, *Science* **353**, 790 (2016).
- [14] F. G. Operti, E. Pugliese, J. S. Andrade, L. Pietronero, and A. Gabrielli, Dynamics in the fitness-income plane: Brazilian states vs world countries, *PLoS ONE* **13**, e0217034 (2018).
- [15] M. Cristelli, A. Gabrielli, A. Tacchella, G. Caldarelli, and L. Pietronero, Measuring the intangibles: A metrics for the economic complexity of countries and products, *PLoS ONE* **8**, 10.1371/journal.pone.0070726 (2013).
- [16] M. Girvan and M. E. J. Newman, Community structure in social and biological networks, *Proc. Natl. Acad. Sci. U. S. A.* **99**, 7821 (2002).
- [17] H. Bathelt, A. Malmberg, and P. Maskell, Clusters and knowledge: local buzz, global pipelines and the process of knowledge creation, *Prog. Hum. Geog.* **28**, 31 (2004).
- [18] T. P. Peixoto, Efficient monte carlo and greedy heuristic for the inference of stochastic block models, *Phys. Rev. E* **89**, 012804 (2014).
- [19] W. Bialek, *Biophysics: searching for principles* (Princeton University Press, 2012).
- [20] S. Cocco, S. Leibler, and R. Monasson, Neuronal couplings between retinal ganglion cells inferred by efficient inverse statistical physics methods, *Proc. Natl. Acad. Sci. U. S. A.* **106**, 14058 (2009).
- [21] G. Tkacik, E. Schneidman, M. J. B. I. au2, and W. Bialek, Spin glass models for a network of real neurons (2009), arXiv:0912.5409 [q-bio.NC].
- [22] J. Shlens, G. D. Field, J. L. Gauthier, M. I. Grivich, D. Petrusca, A. Sher, A. M. Litke, and E. J. Chichilnisky, The structure of multi-neuron firing patterns in primate retina, *J. Neurosci.* **26**, 8254 (2006).

- [23] A. Tang, D. Jackson, J. Hobbs, W. Chen, J. L. Smith, H. Patel, A. Prieto, D. Petrusca, M. I. Grivich, A. Sher, P. Hottowy, W. Dabrowski, A. M. Litke, and J. M. Beggs, A maximum entropy model applied to spatial and temporal correlations from cortical networks in vitro, *J. Neurosci.* **28**, 505 (2008).
- [24] T. Mora, S. Deny, and O. Marre, Dynamical criticality in the collective activity of a population of retinal neurons, *Phys. Rev. Lett.* **114**, 078105 (2015).
- [25] N. Lotfi, A. J. Fontenele, T. Feliciano, L. A. Aguiar, N. A. D. Vasconcelos, C. Soares-Cunha, B. Coimbra, A. J. Rodrigues, N. Sousa, M. Copelli, and P. V. Carelli, Signatures of brain criticality unveiled by maximum entropy analysis across cortical states, *Phys. Rev. E* **102**, 012408 (2020).
- [26] M. L. Ioffe and M. J. Berry II, The structured ‘low temperature’ phase of the retinal population code, *PLoS Comput. Biol.* **13**, e1005792 (2017).
- [27] F. Morcos, A. Pagnani, B. Lunt, A. Bertolino, D. S. Marks, C. Sander, R. Zecchina, J. N. Onuchic, T. Hwa, and M. Weigt, Direct-coupling analysis of residue coevolution captures native contacts across many protein families, *Proc. Natl. Acad. Sci. U. S. A.* **108**, E1293 (2011).
- [28] M. Weigt, R. A. White, H. Szurmant, J. A. Hoch, and T. Hwa, Identification of direct residue contacts in protein-protein interaction by message passing, *Proc. Natl. Acad. Sci. U. S. A.* **106**, 67 (2009).
- [29] R. R. Stein, D. S. Marks, and C. Sander, Inferring pairwise interactions from biological data using maximum-entropy probability models, *PLoS Comput. Biol.* **11**, e1004182 (2015).
- [30] T. R. Lezon, J. R. Banavar, M. Cieplak, A. Maritan, and N. V. Fedoroff, Using the principle of entropy maximization to infer genetic interaction networks from gene expression patterns, *Proc. Natl. Acad. Sci. U. S. A.* **103**, 19033 (2006).
- [31] J. W. Locasale and A. Wolf-Yadlin, Maximum entropy reconstructions of dynamic signaling networks from quantitative proteomics data, *PLoS ONE* **4**, e6522 (2009).
- [32] W. Bialek, A. Cavagna, I. Giardina, T. Mora, E. Silvestri, M. Viale, and A. M. Walczak, Statistical mechanics for natural flocks of birds, *Proc. Natl. Acad. Sci. U. S. A.* **109**, 4786 (2012).
- [33] W. Bialek, A. Cavagna, I. Giardina, T. Mora, O. Pohl, E. Silvestri, M. Viale, and A. M. Walczak, Social interactions dominate speed control in poising natural flocks near criticality, *Proc. Natl. Acad. Sci. U. S. A.* **111**, 7212 (2014).

- [34] K. Burleson-Lesser, F. Morone, P. DeGuzman, L. C. Parra, and H. A. Makse, Collective behaviour in video viewing: A thermodynamic analysis of gaze position, *PLoS ONE* **12**, 1 (2017).
- [35] D. Torres, W. R. Sena, H. A. Carmona, A. A. Moreira, H. A. Makse, and J. S. Andrade, Eye-tracking as a proxy for coherence and complexity of texts, *PLoS ONE* **16**, e0260236 (2021).
- [36] T. Bury, A statistical physics perspective on criticality in financial markets, *J. Stat. Mech.* **2013**, P11004 (2013).
- [37] T. Mora and W. Bialek, Are Biological Systems Poised at Criticality?, *J. Stat. Phys.* **144**, 268 (2011).
- [38] M. da Fazenda, Portal da nota fiscal eletrônica (2003), accessed 2023-05-12.
- [39] M. A. Fischler and R. C. Bolles, Random sample consensus, *Commun. ACM* **24**, 381 (1981).
- [40] O. Chum and J. Matas, Optimal randomized ransac, *IEEE Trans. Pattern Anal. Mach. Intell.* **30**, 1472 (2008).
- [41] M. E. Newman, Analysis of weighted networks, *Phys. Rev. E* **70**, 9 (2004).
- [42] A. Barrat, M. Barthélemy, R. Pastor-Satorras, and A. Vespignani, The architecture of complex weighted networks, *Proc. Natl. Acad. Sci. U. S. A.* **101**, 3747 (2004).
- [43] M. Rubinov and O. Sporns, Complex network measures of brain connectivity: Uses and interpretations, *NeuroImage* **52**, 1059 (2010).
- [44] S. Boccaletti, G. Bianconi, R. Criado, C. I. del Genio, J. Gómez-Gardeñes, M. Romance, I. Sendiña-Nadal, Z. Wang, and M. Zanin, The structure and dynamics of multilayer networks, *Phys. Rep.* **544**, 1 (2014).
- [45] M. Rosvall and C. T. Bergstrom, Maps of random walks on complex networks reveal community structure, *Proc. Natl. Acad. Sci. U. S. A.* **105**, 1118 (2008).
- [46] M. Rosvall and C. T. Bergstrom, Multilevel compression of random walks on networks reveals hierarchical organization in large integrated systems, *PLoS ONE* **6**, e18209 (2011).
- [47] T. Alzahrani and K. J. Horadam, Community detection in bipartite networks: Algorithms and case studies, in *Complex Systems and Networks: Dynamics, Controls and Applications*, edited by J. Lü, X. Yu, G. Chen, and W. Yu (Springer Berlin Heidelberg, 2016) pp. 25–50.
- [48] M. M. S. Nasser and M. Vuorinen, Conformal invariants in simply connected domains, *Lect. Notes. Math.* **20**, 747 (2020).

- [49] N. Papamichael and C. A. Kokkinos, Two numerical methods for the conformal mapping of simply-connected domains, *Comput. Methods Appl. Mech. Eng.* **28**, 285 (1981).
- [50] S. Fortunato and D. Hric, Community detection in networks: A user guide, *Phys. Rep.* **659**, 1 (2016).
- [51] A. B. Bernard, S. J. Redding, and P. K. Schott, Comparative advantage and heterogeneous firms, *Rev. Econ. Stud.* **74**, 31 (2007).
- [52] E. Schneidman, M. J. Berry, R. Segev, and W. Bialek, Weak pairwise correlations imply strongly correlated network states in a neural population, *Nature* **440**, 1007 (2006).
- [53] G. Tkačik, O. Marre, D. Amodei, E. Schneidman, W. Bialek, and M. J. Berry, Searching for collective behavior in a large network of sensory neurons, *PLoS Comput. Biol.* **10**, e1003408 (2014).
- [54] G. Tkačik, T. Mora, O. Marre, D. Amodei, S. E. Palmer, M. J. Berry, and W. Bialek, Thermodynamics and signatures of criticality in a network of neurons, *Proc. Natl. Acad. Sci. U. S. A.* **112**, 11508 (2015).
- [55] W. Bialek, A. Cavagna, I. Giardina, T. Mora, O. Pohl, E. Silvestri, M. Viale, and A. Walczak, Social interactions dominate speed control in driving natural flocks toward criticality, *Proc. Natl. Acad. Sci. U. S. A.* **111**, 7212 (2013).
- [56] H. C. Nguyen, R. Zecchina, and J. Berg, Inverse statistical problems: from the inverse ising problem to data science, *Adv. Phys.* **66**, 197 (2017).
- [57] F. Ataliba, F. D. Barreto, A. Sarquis, and B. D. Menezes, *Desenvolvimento econômico do Ceará: Evidências recentes e reflexões* (2014).